

RECONSTRUCTION OF THE AEROSOL MICROPHYSICAL CHARACTERISTICS AND OZONE CONCENTRATION FROM SATELLITE OBSERVATIONS OF THE SUN

V.V. Butov and S.V. Loginov

*Scientific-Industrial Association "Energiya", Moscow
Design and Technological Institute "Optika",
Siberian " ranch of the Russian Academy of Sciences, Tomsk
Received January 11, 1995*

Technique is proposed for reconstructing stratospheric ozone concentration, as well as aerosol extinction coefficient and microphysical parameters, which is based on direct solar radiation attenuation measurements using Spectr-256 multichannel spectrometer onboard a satellite. Separation between ozone and aerosol optical thicknesses is accomplished with Angström approximation of spectral dependence of the aerosol extinction coefficient in 0.45–0.83 μm wavelength range, while the profile reconstruction employs Tikhonov method of generalized discrepancy. For assumed aerosol type and altitude profile of aerosol refractive index, particle size distribution function is calculated for each altitude, as well as aerosol particle mean radius and size distribution width.

There is a number of methods for observation of atmospheric ozone and aerosol, usually employing either balloon and aircraft measurements, or satellite and ground-based sensing. All these are in common use now to treat many problems of atmospheric photochemistry and dynamics. Global monitoring of the atmospheric constituents was accomplished by means of satellite instruments such as SBUV, LIMS, SAM, and SAGE.¹ These instruments were used to study El-Chichon and Pinatubo eruptions, to monitor ozone holes over Antarctic continent, and to detect stratospheric particles in polar regions. However, the above-mentioned instruments have poor spatial resolution, insufficient to treat fine structure in admixture distributions.

This drawback was partially overcome with SAGE-II device used to continue experiments started with SAM and SAGE. The SAGE-II is a 7-channel photometer measuring atmospheric transmission in the visible and near-IR ranges of the spectrum. Additionally, a method was devised² capable of reconstructing the vertical ozone profile to an accuracy of 10% in 10–50 km altitude range, while allowing accurate reconstruction of aerosol extinction coefficient profile between 10- and 20-km altitude. Chosen altitudinal step was 1 km. Parameterization of the aerosol size distribution functions was used to calculate aerosol microphysical characteristics.

OZAFS experiment (ozone and aerosol fine structure) was conducted in 1985 onboard the Salut-7

satellite.¹ During this experiment, measurement of atmospheric extinction of solar radiation was combined with photographic observations of the Earth's aureole in twilight. The experiment has continued study of stratus-like structure of twilight aureole initiated in 1977-1978 on the Salut-4 space station which had revealed coloring of twilight aureole over the near-horizon sky area; the horizon coloring had nonuniform pattern as thin layers of different colors. Such a stratus-like structure of aureole is due to increasing ozone and aerosol concentrations, as was confirmed numerically in Ref. 1. In the stratosphere the layer structure comprises the ozone and aerosol layers, while in the troposphere it is due to aerosol layers. In OZAFS experiment the aerosol and ozone spatial characteristics were determined with 5–10% accuracy and 1-km resolution. The device was operated at 4 spectral channels, that required the introduction of rigid *a priori* assumption on spectral dependence of aerosol extinction coefficient. The reduction technique was applied to reconstruct ozone concentration and aerosol extinction coefficient vertical profiles, that (as in the statistical regularization technique) uses covariation matrices of ozone partial pressure and aerosol extinction; therefore, measurements collocated with data of the matrices were needed.

The use of multichannel spectrometers, such as Spektr-256, Gemma-2, HRIS, operating at the same wavelength range as SAGE-II, allows us 1) to obtain aerosol microphysical characteristics without resorting

to a parameterization of aerosol particle size distribution function; 2) to identify and calculate, with less error, the concentration of gaseous species whose absorption bands are in the visible and near-IR. The spatial resolution at horizon is 500 m for Spektr-256 and Gemma-2, and 150 m for HRIS. The altitude step is 70 m. With the advent of multichannel spectrometers like those just described, much more reliable and accurate study of fine spatial structure of atmospheric constituents is now feasible.

The present work is an attempt to solve problem on reconstructing vertical profiles of aerosol extinction coefficient, $\beta^a(h)$, some aerosol microphysical parameters, and ozone concentration, $N_o(h)$, from the data of passive sensing from space. Direct solar radiation attenuation was measured. The receiving spectrophotometer was mounted on the Mir space station. For the chosen geometry of the experiment, it was possible to apply Bouguer law, within which the measured intensity $I_\lambda(h)$ and the atmospheric optical depth $\tau_\lambda(h)$ are related simply as

$$I_\lambda(h) = S_\lambda e^{-\tau_\lambda(h)}, \quad (1)$$

where S_λ is the solar constant; $\tau_\lambda(h) = \tau_\lambda^r(h) + \tau_\lambda^a(h) + \tau_\lambda^o(h)$; $\tau_\lambda^r(h)$, $\tau_\lambda^a(h)$, $\tau_\lambda^o(h) = \chi K_\lambda$ are the Rayleigh, aerosol, and ozone optical depths, respectively; K_λ is the ozone absorption cross section, χ is the path-integrated ozone concentration.

Because the value of $\tau_\lambda^r(h)$ at altitudes above 15-km is within 3% of the Rayleigh depth corresponding to the standard atmosphere, a standard atmospheric model can be used to determine Rayleigh depth. Hence, only two parameters, $\tau_\lambda^a(h)$ and $\tau_\lambda^o(h)$, are to be determined. Within the instrument operational range, 0.45–0.83 μm , the ozone absorption can be assumed to occur mainly in the Chappuis 0.53–0.73 μm band, while aerosol depth dependence on wavelength is given by the Angström formula,³ namely

$$\tau_\lambda^a = \tau_{\lambda_0}^a \left(\frac{\lambda_0}{\lambda} \right)^v. \quad (2)$$

Thus, by deriving aerosol depth at 0.45–0.83 μm band, and interpolating it, using Eq. (2), to Chappuis band, one can obtain ozone depth. Similar procedure was used in Refs. 1 and 4 to reconstruct $\beta^a(h)$ and $N_o(h)$ from photos of the setting Sun. The photographs were taken at four spectral channels. For this reason, the authors of Refs. 1 and 4 proceeded with a fixed v value for the aerosol structure suggested. By contrast, the $\tau_\lambda^a(h)$ value and the exponent v herein are those derived from the measured depth $\tau_\lambda(h)$.

1. DETERMINATION OF AEROSOL DEPTH $\tau_\lambda^a(h)$

Assuming $\tau_\lambda^a(h)$ and v to be parameters, one can construct the functional

$$F(\zeta, v) = \sum_i \left[\ln \tilde{\tau}_{\lambda_i}(h) - \left(\zeta + v \ln \left(\frac{\lambda_0}{\lambda_i} \right) \right) \right]^2,$$

where λ_0 is a reference wavelength, $\tilde{\tau}_{\lambda_i} = \tau_{\lambda_i} - \tau_{\lambda_i}^r$; $\zeta = \ln(\tau_{\lambda_0}^a(h))$.

Then parameters ζ and v follow from condition

$$F(\zeta, v) \xrightarrow{\zeta, v} \min. \quad (3)$$

Equation (3) can be solved in a number of ways. Specifically, we applied simplex and gradient techniques of minimizing Eq. (3) (see Ref. 5) imposing explicit restriction,

$$-11 \leq \zeta \leq 1, \quad 0 \leq v \leq 7.$$

Here restrictions on ζ and v are based on literature data on the existing optical models of the atmosphere.^{6–8} To check a global minimum, Ref. 5 recommends searching for a minimum at several initial points. Accordingly, we specified initial points on a grid formed by simply dividing intervals. From the set of values thus obtained, we then selected those pairs (ζ, v) forming domain \mathbf{G} with the largest density of solutions. The size of domain \mathbf{G} , giving the required accuracy of solving the functional (3), is evaluated by model calculation to be 0.15. The sought ζ and v were finally taken averaged over \mathbf{G} .

We took rms deviations $\delta\zeta$ and δv as estimates of possible error in the ζ and v determination. For ζ and v reconstructed from the model $\tilde{\tau}_\lambda$ values, the errors $\delta\zeta$ and δv were within 1%. Addition to $\tilde{\tau}_\lambda$ from uncorrelated noise with an amplitude equal to 50% of $\tilde{\tau}_\lambda$ increased $\delta\zeta$ to 5% and δv to 10%. Change in noise correlation length from 1 to $L/3$ (L is the number of spectral channels used to calculate (3)) produced further threefold increase of the errors, $\delta\zeta \approx 15\%$ and for $\delta v \approx 45\%$.

The ζ and v values thus obtained were then used to extrapolate to Chappuis band, and to calculate the ozone depth τ_λ^o afterward. Given τ_λ^o and the absorption cross-section K_λ linearly related, the least squares method is the most standard to calculate the integrated concentration χ . The error $\delta\chi$, defined as rms deviation herein was within 10% for a 50% noise added.

2. RECONSTRUCTION OF VERTICAL PROFILES OF AEROSOL EXTINCTION COEFFICIENT AND OZONE CONCENTRATION

The problem of reconstructing aerosol extinction coefficient $\beta^a(h)$ and ozone concentration $N_o(h)$ from measured depths was solved applying regularization techniques.^{9,10} For the viewing geometry adopted, the dependence of $\beta^a(h)$ on $\tau^a(h)$ can be represented as a linear matrix equation of the form

$$\tau^a = \mathbf{B} \beta^a + \xi, \quad (4)$$

where ξ is the measurement error. Elements of the matrix \mathbf{B} are the segments of optical path, on which $\beta^a(h)$ values remain unchanged. Similar expression can be written to relate altitude distribution of ozone, $N_o(h)$, to the path-integrated ozone concentration, χ .

Since the calculated matrix \mathbf{B} is rectangular, the generalized discrepancy technique^{9,10} can be applied to solve Eq. (4). Reconstruction error was estimated by the method from Ref. 10 as

$$\sigma_i = \left(\sqrt{(\mathbf{C} + \alpha\Omega)^{-1}} \right)_{ii}$$

$$\mathbf{C} = \mathbf{B}^+ \mathbf{W} \mathbf{B}, \quad W = \frac{\delta_{ij}}{\omega_i \omega_j}, \quad i = 1, \dots, N, \quad j = 1, \dots, N,$$

where Ω is the second-order stabilizer, α is the unknown Lagrange factor, ω_j is the rms error of $\tau^a(h)$ measurement at an altitude h_j , N is the total number of nodes in the solution being reconstructed.

3. DETERMINATION OF PARTICLE SIZE SPECTRUM

Particle size distribution was determined by a technique from Ref. 11. We processed those aerosol optical depths measured outside the Chappuis band, within 0.45–0.53 μm and 0.75–0.83 μm intervals. All in all, 60 spectral channels were used in the calculations. Following the argument in Ref. 11, we write down

$$\tau_\lambda^a(h) = \int_h^H \int_0^{\$} \pi r^2 Q(r, \lambda, m) f(r, h') \, d r \, dl(h') \approx$$

$$\approx \pi H_d \int_{r_0}^{r_f} \pi r^2 Q(r, \lambda, m) f(r, h) \, d r, \quad (5)$$

where $f(r, h)$ is the particle size distribution function, $Q(r, \lambda, m)$ is the extinction efficiency factor calculated using Mie theory for spherical homogeneous particles with radius r and complex refractive index m , H_d is the aerosol altitude scale, $dl(h')$ is an element of beam path, h' is an altitude of the viewing line perigee.

In the experiment, we calculated the extinction efficiency factor $Q(r, \lambda, m)$ for a medium of spherical particles with a nearly unit refractive index m (Ref. 12), namely by the formula

$$Q(\rho) = 2 - \frac{4}{\rho} \sin(\rho) + \frac{4}{\rho^2} (1 - \cos(\rho)),$$

where $\rho = 2(m-1)(2\pi r/\lambda)$.

Conversion of Eq. (5) into its finite-difference analogue gives a linear matrix relation between τ_λ^a and $f(r, h)$.

In the wavelength regions used, the matrix Q is poorly stipulated, i.e. its determinant $\det Q \approx 0$. Therefore, imposition of weak uncorrelated perturbations on the extinction factor, such that $\|Q - \tilde{Q}\| \ll \infty$ (\tilde{Q} is the perturbed matrix) allows the problem to be reduced to the solution of Eq. (5) with inaccurately preset matrix \tilde{Q} . Then the approximate normal solution $\tilde{f}(r)$, converging to exact solution $f(r)$, can be found by means of regularization algorithm.⁹ The calculational error was determined with the help of technique, described in Section 2.

Model estimates show that, for the spectral intervals chosen, the addition of white noise at a level of 10% of τ_λ^a value will limit the satisfactory reconstruction of $f(r)$ distribution to 0.1–3 μm .

Aerosol microphysical characteristics, such as mean particle size $\langle r \rangle$ and the size distribution width δr were calculated as the mean and rms deviation from the distribution $g(r, h) = r f(r, h)$ normalized to the total number of particles in the size range of 0.1–3 μm .

4. ATMOSPHERIC SENSING DATA

Atmospheric attenuation of solar radiation was measured by spectrophotometer with the following features: operational range is from 0.45 to 83 μm , the number of spectral channels is 128/256 with widths of 3/1.5 nm, respectively. To make the entire operational range available for measurements, a complex filter was used, assembled with glasses of HC11 and 3C8 types. Change of solar brightness S_λ , due to viewing line (VL) travel from the Sun's disk center to the edge, was modeled as in Ref. 13.

Given the essentially nonuniform solar brightness across the Sun's disk, the VL position relative to the Sun's disk center is important. A VL travel due to refraction was treated with a standard refraction model from Ref. 14. The VL displacement due to permanent motion of the station was quantified for a high-elevated Sun from brightness variation at the shortwave edge of the spectrum. The performed photo control tie has made it possible to get the angular separation between VL and the direction to the Sun center, located at the altitude $h \approx 26$ km; that was done based on the apparent Sun disk deformation due to

refraction. With the above factors properly accounted, the VL travel on the Sun disk was controlled with the accuracy no less than 1', translated to roughly 5% error in brightness measurements comparable with the instrument inherent noise.

Spectral measurements of the setting Sun were performed on April 16, 1992 from Mir space station. During the experiment, the perigee of the viewing line was located over 48.6°S and 27°W.

The above method (see Sections 1-3) of processing the measured optical depths was used to derive altitude profiles of aerosol extinction coefficient $\beta^a(h)$ (reference wavelength $\lambda_0 = 0.79 \mu\text{m}$), ozone concentration $N_o(h)$, mean radius of aerosol particles $\langle r(h) \rangle$, and aerosol particle size distribution width $\delta r(h)$ (Figs. 1, 2, and 4). Simple running averaging was applied to smooth the calculational results over scale corresponding to the instrument spatial resolution, specifically, over $\sim 0.5 \text{ km}$, for geometry adopted. The δr calculation used refractive index models from Refs. 15 and 16. The estimates for $\langle r(h) \rangle$ and δr (Fig. 2) were calculated based on the data presented in Ref. 17 for 20 km altitude.

Figure 3 is the contour plot showing altitude distribution of aerosol particles in size range of 0.1 to 5 μm . For convenience, the function $\log[g(r, h)]$ was calculated for values normalized to a unit interval at each altitude level. The plotting was made on a 30x30 grid.

In Figs. 1-3, five distinct aerosol layers are identified:

13-19 km altitude range. This is the layer having maximum value of the extinction coefficient $\beta^a(h)$ equal to $3 \cdot 10^{-3} \text{ km}^{-1}$. Aerosol particles in this layer have mean radius $\langle r(h) \rangle \sim 0.38-0.45 \mu\text{m}$ and rms deviation $\delta r(h) \sim 0.35 \mu\text{m}$ (Fig. 2).

20-22 km. The layer is composed of nearly equal-sized particles with the radius $\langle r(h) \rangle \sim 0.55-0.65 \mu\text{m}$ and rms deviation $\delta r(h) \sim 0.3 \mu\text{m}$. It shows little nonuniformity in vertical, being almost unresolved into sublayers (Figs. 1 and 2).

32 and 36 km. The middle of the layer is composed of particles with the radius $\langle r(h) \rangle \sim 0.32 \mu\text{m}$, while its top and bottom are dominated by particles with $\langle r(h) \rangle \sim 0.5 \mu\text{m}$. The rms deviation $\delta r(h) \sim 0.38 \mu\text{m}$ throughout.

34 km. Quite a uniform layer with particles 0.53 μm in radius. The aerosol population is not distinctly stratified, as in a 20-22 km layer.

42.5 km. It is 1-km thick layer made of particles with $\langle r(h) \rangle \sim 0.58 \mu\text{m}$ and $\delta r(h) \sim 0.3 \mu\text{m}$.

In addition, between 24- and 30-km altitudes, aerosol particles in size range of 0.1 to 1 μm are contained in near equal mixing ratios (Figs. 1, 2).

As is evident from the $\log[g(r, h)]$ pattern, aerosol particles typically have unimodal size distribution.

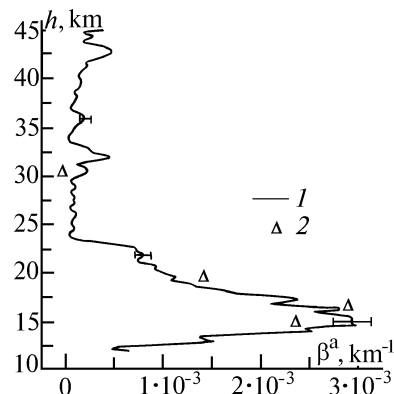


FIG. 1. Altitude profiles of aerosol extinction coefficient, $\beta^a(h)$, for the wavelength of $0.79 \mu\text{m}$: reconstructed one (1) and model⁷ (2).

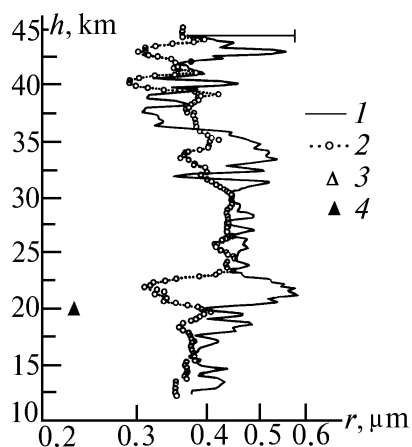


FIG. 2. Altitude profiles of the mean radius, $\langle r(h) \rangle$ (1), and size distribution width, $\delta r(h)$ (2), of aerosol particles, estimates for $\langle r(h) \rangle$ (3) and $\delta r(h)$ (4) at altitude of 20 km from the data of Ref. 17, $\lambda = 0.69 \mu\text{m}$.

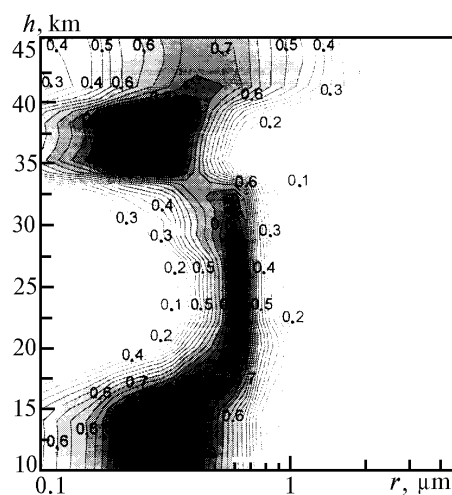


FIG. 3. Contour plot of aerosol particle size distribution in the stratosphere.

The existence of strong amplitude fluctuations in $\langle r(h) \rangle$ and $\delta r(h)$ (Fig. 3) indicates that aerosol is likely arranged in stratospheric layers ≈ 1 km thick. The aerosol stratification is most apparent between 35 and 45 km.

Profile of ozone concentration has two distinct maxima at 22–23 km and 32 km, with values of $4.5 \cdot 10^{18} \text{ m}^{-3}$ and $2.5 \cdot 10^{18} \text{ m}^{-3}$, respectively. Both maxima fall within particle size range of 0.55 to 0.65 μm . For comparison, Fig. 4 presents ozone profile based on model estimates.¹⁸ As seen, retrieved values are within 10% of the model estimates.

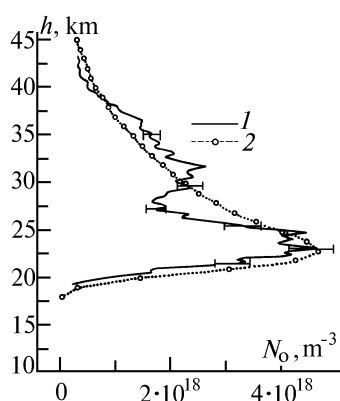


FIG. 4. Altitude profile of the ozone concentration, $N_o(h)$: reconstructed (1) and modeled with MAP (2).

5. CONCLUSION

Summarizing, it can be said that given stratospheric satellite sensing data available for the 0.45–0.83 μm wavelength range, the vertical profiles of aerosol extinction coefficient $\beta^a(h)$ and ozone concentration $N_o(h)$ can be reconstructed using spectrophotometric measurements. Also, the assumptions made for aerosol type and altitude profile of aerosol extinction coefficient has made it possible, for each altitude level (i.e., for each 60–70 m at horizon), to calculate the particle size distribution function $g(r, h)$, and, additionally, to evaluate mean aerosol particle radius $\langle r(h) \rangle$ and size distribution width $\delta r(h)$. The method just described is intended to process results from a series of experiments made within the atmospheric sensing scheme also described herein.

The profiles of ozone concentration, aerosol extinction coefficient and aerosol microphysical parameters, thus reconstructed, can be then used to investigate stratospheric dynamics and to study the interaction of atmospheric constituents.

ACKNOWLEDGMENT

Authors would like to acknowledge Dr. G.M. Grechko for his help in experiments.

REFERENCES

1. G.M. Grechko, N.Ph. Elanskii, et al., "The OZAPS experiment in observing the fine structure of the ozone and aerosol distribution in the atmosphere from the Salut-7 orbital station," Preprint No. 8, Institute of Atmospheric Physics, Moscow (1990), 72 pp.
2. P.-H. Wang and M.P. McCormick, J. Geophys. Res. **94**, D6, 8435-8446 (1989).
3. A. Angstrom, Tellus **XVI**, No. 1, 64-75 (1964).
4. G.M. Grechko, A.S. Gurvich, N.Ph. Elanskii, et al., Dokl. Akad. Nauk SSSR **301**, No. 2, 306-309 (1988).
5. B. Bandi, *Optimization Techniques. Introductory Course* [Russian translation] (Radio i Svyaz', Moscow, 1988).
6. K.Ya. Kondrat'ev, G.I. Marchuk, A.A. Buznikov, et al., *Radiative Field in a Spherical Atmosphere* (State University, Leningrad, 1977), 216 pp.
7. V.E. Zuev and G.M. Krekov, *Current Problems in Physics, Vol. 2, Optical Models of the Atmosphere* (Gidrometeoizdat, Leningrad, 1986), 256 pp.
8. P.B. Russel, T.J. Swisler, et al., J. Atm. Sci. **38**, No. 6, 1279-1294 (1981), 216 pp.
9. A.N. Tikhonov and V.Ya. Arsenin, *Methods of Solving Ill-Posed Problems* (Nauka, Moscow, 1979), 285 pp.
10. V.F. Turchin and V.Z. Nozik, Izv. Akad. Nauk SSSR, Fiz. Atmos. Okeana **5**, No. 1, 29-38 (1989).
11. R. Rizzi, R. Guzzi, and R. Legnani, Appl. Opt. **21**, No. 9, 1578-1587 (1982).
12. H.C. Van de Hulst, *Light Scattering by Small Particles* (Wiley, New York, 1957).
13. G. Kasper, ed., *Solar System, Vol. 1, Sun* [Russian translation] (Foreign Literature Press, Moscow, 1957).
14. G.M. Grechko, A.S. Gurvich, et al., Tr. Gos.Opt. Inst., Leningrad **71**, Iss. 205, No. 1., 121 pp.
15. M.S. Belen'kii, G.O. Zadde, et al., *Optical Model of the Atmosphere*, Tomsk Affiliate of the Siberian Branch of the Academy of Sciences of the SSSR, Tomsk (1987).
16. WCP, Section 2, Boulder, Colorado, USA (1982).
17. J.M. Livingston and P.B. Russel, J. Geophys. Res. **94**, No. D6, 8425-8433 (1989).
18. G.M. Keating and D.F. Young, in: *Handbook for MAP*, Vol. 16, University of Illinois (1985), pp. 205-230.